

Effects of Centrifugal Disc Finishing for Surface Improvements in Additively Manufactured Gears

Foxian Fan^{1*}, Nicholas Soares², Sagar Jalui², Aaron Isaacson³, Aditya Savla¹, Guha Manogharan², and Tim Simpson^{1,2}

¹*Department of Industrial and Manufacturing Engineering, The Pennsylvania State University, University Park*

²*Department of Mechanical Engineering, The Pennsylvania State University, University Park*

³*Applied Research Laboratory Gear Research Institute, The Pennsylvania State University, University Park*

*Corresponding author: fwf5049@psu.edu, The Pennsylvania State University

Abstract

Additive Manufacturing (AM) is well suited to rapidly produce complex and customized geometries economically for low production runs. However, there is an inherent need for post-AM machining and surface finishing in most metal AM applications. Centrifugal Disc Finishing (CDF) is a media-based mass finishing process that can be employed to improve surface finish of external surfaces of AM parts with complex geometry. This original study aims to understand the influence of CDF processing conditions on Ti64 gear teeth fabricated via Powder Bed Fusion (PBF). A detailed statistical analysis is conducted to analyze the effectiveness of CDF to improve surface roughness of different build surfaces of the AM gear teeth. In addition, both contact profilometer and X-ray Computer Tomography (CT) techniques are applied to evaluate its effectiveness to measure CDF and AM surface finishing. Findings from this study on CDF of gear AM will benefit metal AM community by better understanding the impact of CDF processing conditions for surface improvements in mass finishing of metal AM parts.

Keywords: Centrifugal disc finishing; AM surface finishing; AM gears; surface roughness; CT roughness measurements; powder bed fusion

Introduction

In recent years, disruptive development in Additive Manufacturing (AM) has given manufacturers the ability to overcome previous geometric limitations in manufacturing processes. Commercial AM metal products, such as gears and other crucial mechanical components, have begun to be widely adapted to AM production. Although AM offers many benefits in overcoming geometric limitations in different applications, higher geometry complexity has also increased the difficulty and cost in post-finishing procedures. Given this increase, the cost of post-finishing is becoming one of the largest factors in metal Additive

Manufacturing cost. The National Institute of Standards and Technology (NIST) reported that the cost of AM post-processing can range from 4%-13% of the total manufacturing cost, depending on the process [1]. Similarly, Wohlers Report 2019 indicated that “more than 26% of the cost is from post-processing” [2]. Although typical post-processing procedures such as CNC machining provide good precision and surface finish, post-finishing procedures have increased lead time and cost due to low capacity, long setup time, and high machining cost. Furthermore, CNC machining-based tool path planning and tool accessibility also have become a critical limitation in AM designs. As the geometry complexity in AM objects increases, post-processing cost and difficulties increase as well.

Centrifugal Disc Finishing (CDF) is a common type of abrasive media-based mass finishing process for surface finish improvement. Similar mass finishing processes include vibratory bowl, drag finishing, stream finishing, and centrifugal bowl finishing. However, unlike many Mass Finishing processes, CDF does not require any fixtures or additional supports for parts. While the media-based mass finishing processes often require more time than similar machining processes, the setup time, capacity, and ability to handle complex parts can be superior to CNC machining. The primary investigation in the paper is to determine the change in surface roughness of Powder Bed Fusion (PBF) built Ti-64 gear teeth after CDF post-processing, with respect to CDF process parameters.

Literature Review

The CDF machine consists of a stationary barrel with a disc shaped rotor at the bottom of the barrel (Figure 1). While running, the disc rotates at high speed and “the mass within the container is accelerated outward and then upward against the stationary side walls of the container, which act as a brake. The media and parts rise to the top of the load and then flow in toward the center and back down to the disc” [3]. The barrel size, media, and rotational speed vary depending on type of machine and part to be finished. CDF can be operated either with or without lubricant, known as wet or dry, respectively. Kitajima et al. [4] studied how the flow-through system in CDF affects the material removal rate and surface roughness. The lubricant type and flow rate impact were compared in terms of surface roughness and stock removal rate. The experiment finds the highest flow rate result in lowest surface roughness in comparison to lower flow rate and batched lubricant. Furthermore, stock removal rate is the highest when flow rate is set at lowest. According to user manual of Walther Trowal TT45 Centrifugal Disc Unit, key parameters of the CDF include media size, rotational speed, and lubricant concentration. Matsumoto et al. [5] investigated distribution of flow pressure of the media under both dry and wet conditions. The results showed that the bottom half of the barrel exhibited higher pressure under both conditions, and the stock removal in the dry processes was greater than that of the wet process.

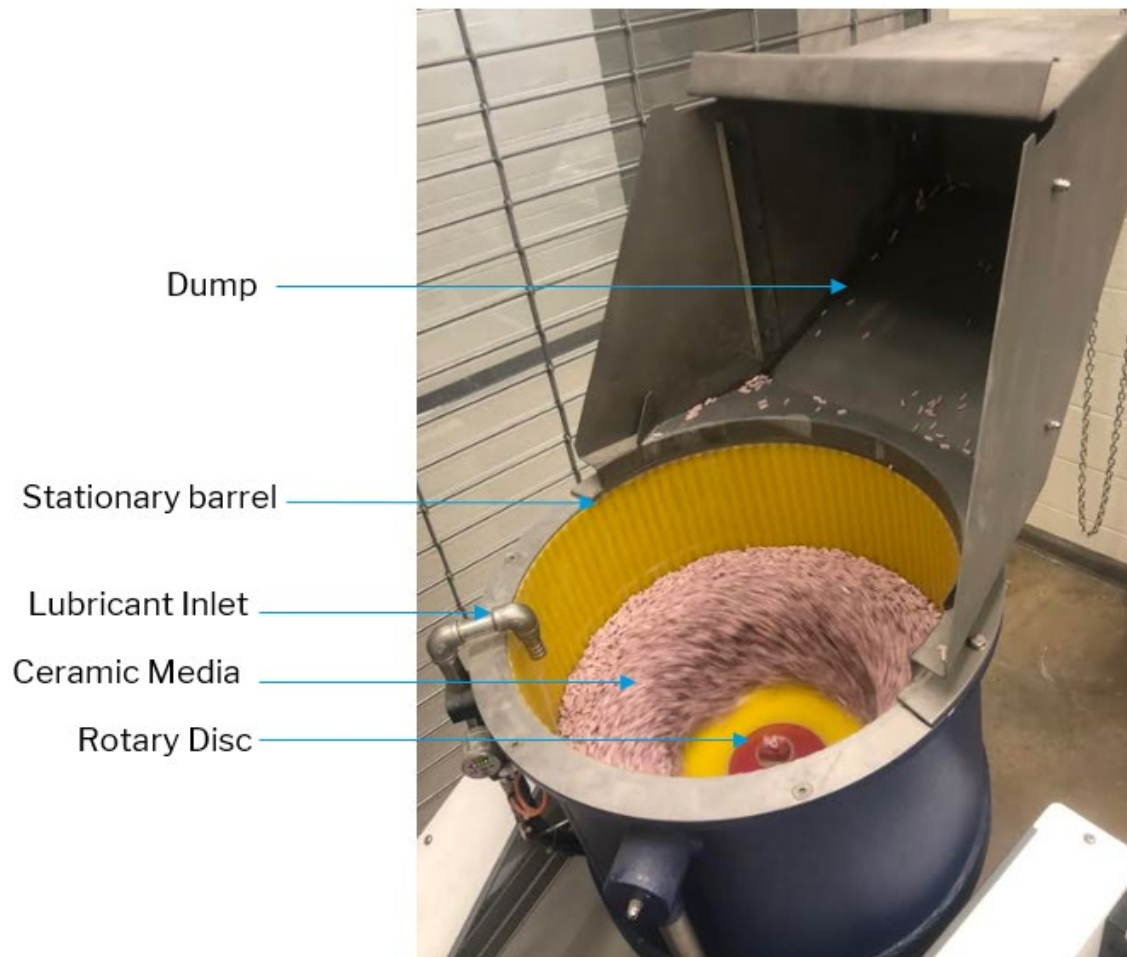


Figure 1. Walther Trowal TT45 Centrifugal Disc Finishing Unit

Furthermore, mechanical simulations have been conducted for centrifugal disc finishing. Sutowski et al. [6, 7] simulated the media flowing mechanism of centrifugal disc finishing. The result determined that the media in the bottom half of the barrel had higher velocity and energy. Cariapa et al. [8] developed a material removal rate prediction model for CDF with spherical ceramic media. The main predictors consist of the density ratio and hardness ratio of testing metal and media. The most appropriate exponential fitted model exhibited a maximum of 16% deviation. Although studies in CDF material removal rate or surface roughness prediction models are scarce, prediction models and for vibratory finishing processes have been studied through a few approaches including experiment based approach, surface geometry based approach, discrete element analysis, and computational fluid dynamics analysis, [9–12]. Vijayaraghavan et al. [13] summarized literatures on varieties of mass finishing studies and conducted an experiment using a vibratory finishing process. A model for Ra (arithmetic mean) surface roughness based on media shape, conical and cylindrical, was developed and tested with input parameters consisting of orientation, lubricant concentration, and processing time.

Jamal & Morgan [14] conducted an experiment to test surface roughness improvement effectiveness on Selective Laser Melting (SLM) fabricated Ti-64 samples. Subjects are tested through drag finishing, stream finishing, high energy centrifugal barrel finishing, and centrifugal disc finishing. Although the centrifugal disc was found to be the least efficient in comparison to the other processes, the author stated that the media type used in this study was not optimal. Boschetto et al. [15] conducted an investigation on using Centrifugal Barrel Finishing to process SLM fabricated Ti-64 parts. This study considered stratification angle, rotational speed, and processing time as parameters that affected resultant surface roughness. The result indicated that 90-degree stratification angle specimens are harder to process than 0-degree specimens, while 45-degree specimens had medium behavior. Overall, there exist few studies in CFD application for post-processing AM parts. In this paper, the effect of CDF process parameters on the surface roughness of Ti-64 AM parts is examined and statistically analyzed to investigate applicability of CDF in metal AM post-processing.

Methods

Experiment Setup

The 3D-printer used in this experiment was the 3D Systems Prox DMP 320 Powder Bed Fusion printer. The powder used was Ti6Al4V (Grade 23) with a nominal size of 15-45 micrometer. A total of 21 gear teeth samples were printed, each consisting of one and a half teeth (Figure 2). The nominal dimensions of the samples were $0.44 \times 0.45 \times 0.50 \text{ mm}^3$ (Figure 3). The gear teeth were built vertically along the Z-direction, which was perpendicular to build plate, as seen in Figure 2. Each sample number was directly printed onto the structure using a boss on the top face (Figure 4). The support structure was manually scraped off the build plate and the samples did not undergo heat treatment or any other post-processing techniques before the CDF process.

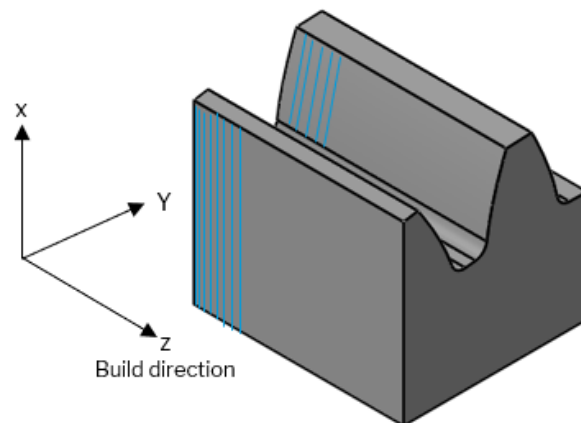


Figure 2. CAD model of the gear tooth samples used in this study, including build direction

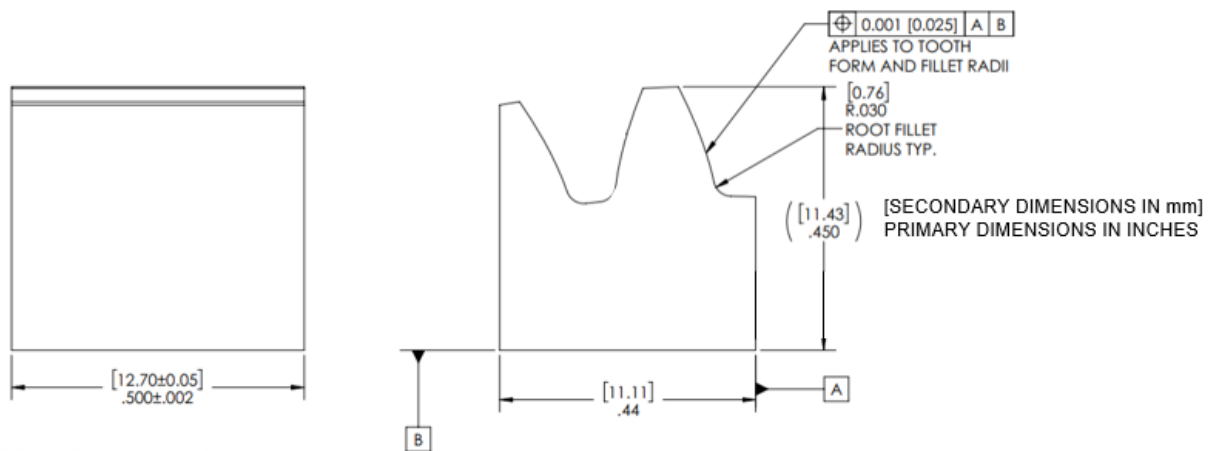


Figure 3. Dimensioned drawing of the gear teeth samples

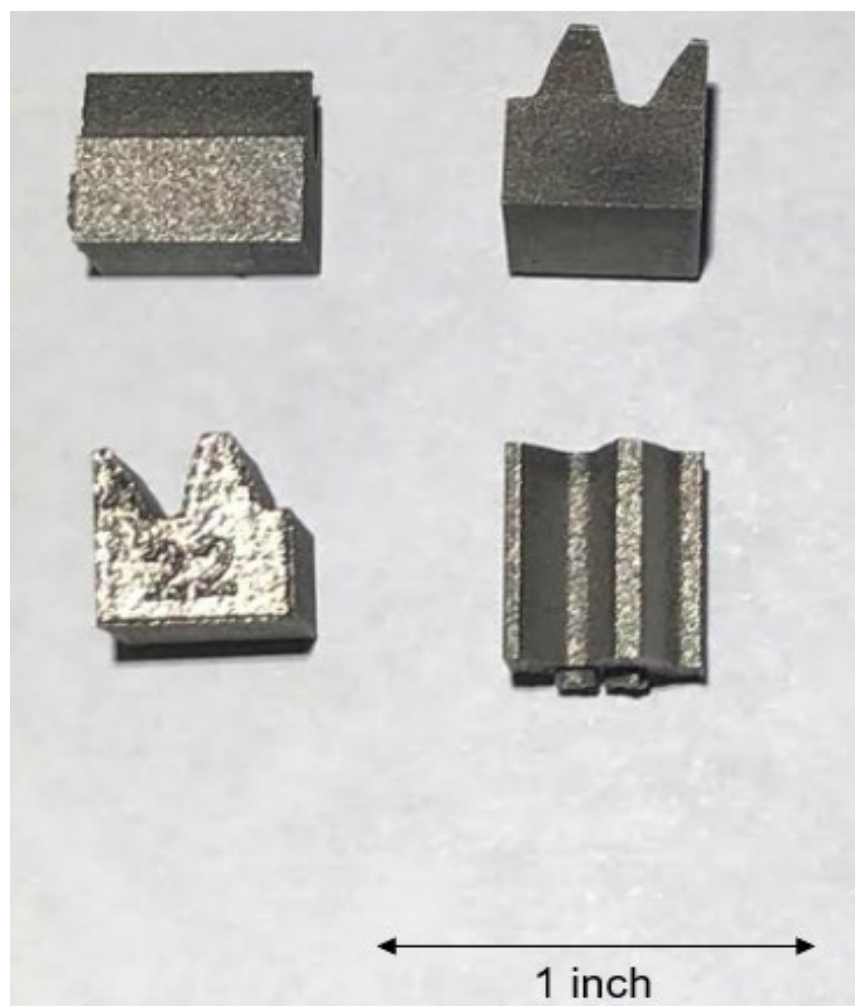


Figure 4. Various views of the as-printed gear teeth samples

CDF Machine Parameters

The focus of this study was on investigating how rotational speed (RPM) and processing time (minutes) of the CDF process affect the surface roughness of the samples. The triangular ceramic media used is shown in Figure 5, with nominal dimensions of 4 mm x 10 mm. The loading ratio, lubricant flow rate, and finishing media remained fixed throughout the experiment. 18 of the samples were processed under six different conditions, in groups of three, and compared to the remaining three control (as-built) samples (Table 1).

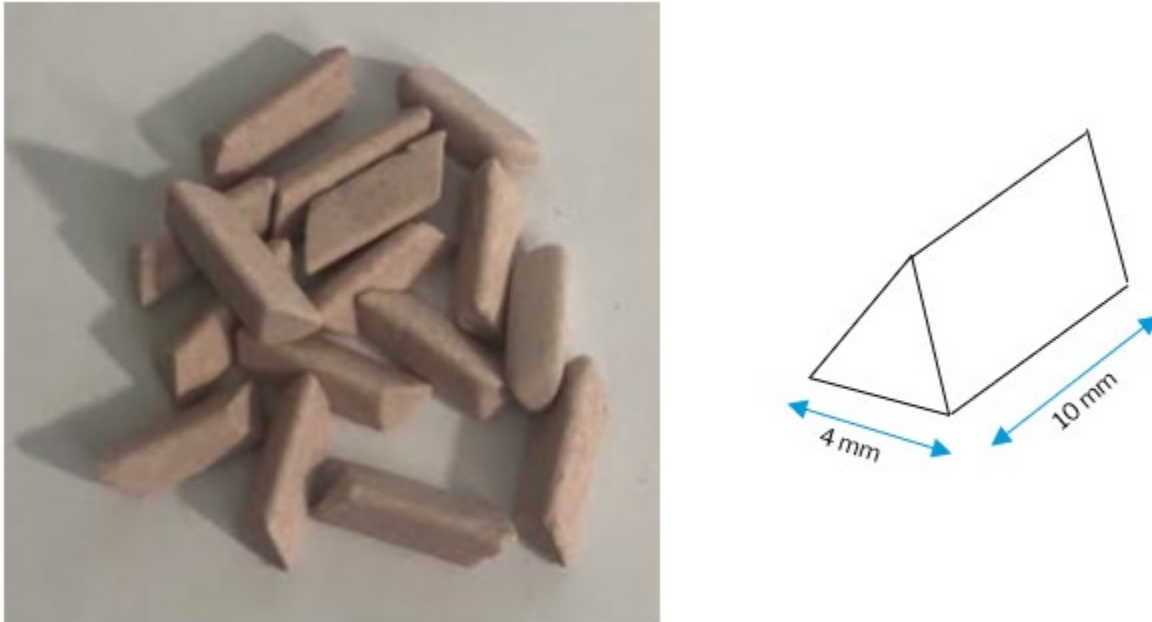


Figure 5. Triangular ceramic media used in CDF, with nominal dimensions of 4 mm x 10 mm

Table 1. CDF processing conditions for each gear teeth sample, including the processing speed (RPM) and duration (minutes).

Sample Number	CDF Processing Conditions
1, 2, 3	15 minutes, 200 RPM
4, 5, 6	30 minutes, 200 RPM
7, 8, 9	60 minutes, 200 RPM
10, 11, 12	30 minutes, 150 RPM
13, 14, 15	30 minutes, 250 RPM
16, 17, 18	30 minutes, 280 RPM
19, 20, 21	None

Surface Profilometer Data Acquisition

A Taylor-Hobson Surtronic S128 profilometer was used to collect the surface roughness data for five different directions on each sample, shown in Figure 6. Directions 1 and 2 are along exterior face of the sample, parallel and perpendicular to the build direction, respectively. Directions 3

and 4 are along the interior tooth profile, parallel and perpendicular to the build direction, respectively. Direction 5 is along the exterior tooth profile, perpendicular to the build direction. While the most common roughness measurements in gear teeth analysis are taken along the tooth profile (directions 4 and 5), these five directions allow for the comparison of the CDF finishing capabilities in multiple areas. The first area of interest is the comparison of surface roughness for features parallel and perpendicular to the build layers. Next, the difference in roughness of external and internal features can be investigated. Finally, the surface profiles of flat faces can be compared to those of curved features. According to a review by Townsend et al. [16], ISO 4287 arithmetic mean (R_a) surface roughness is the most widely used surface metrology benchmark in AM literature. In this study, both arithmetic mean surface roughness (R_a) and mean roughness depth (R_z) were evaluated statistically and determine the relationship between processing time, rotational speed, and surface roughness.

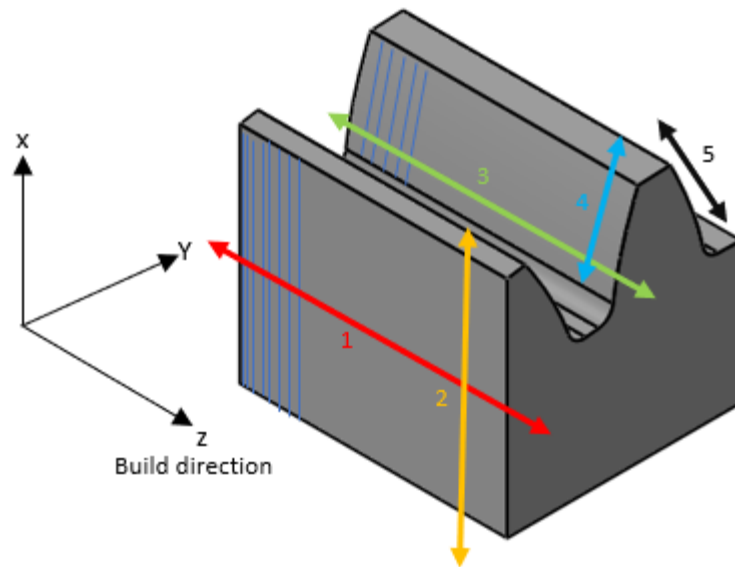


Figure 6. CAD model of gear teeth sample, showing the five directions used for surface roughness measurements

Surface Inspection Using Micro-CT

Micro-CT scans were obtained using a General Electric v|tome|x L300 nano/microCT scanner. In order to capture the data of small features, a voxel size of 11 μm was chosen. The raw scan data was imported into ImageJ. The stack was converted to 8-bit from 32-bit for ease of data handling. Processed image files were then transferred to Avizo for 3D image reconstruction.

Discussion and Analysis

Individual Surface Regression Results (R_a)

The individual surface roughness data (R_a) collected for each group of test variable combinations can be seen in Figures 7-11. The R_a surface roughness linear regression result for

Directions 1, 2, and 4 showed that rotational speed (RPM) was a significant parameter, at $\alpha=0.05$ significance level (Figures A1, A2, and A4), but not significant for profiles 3 and 5 (Figures A3, A5). The parameter time (minutes) is not a significant parameter for all surfaces, using a $\alpha=0.05$ significance level. The boxplots trends indicate external surfaces (Directions 1,2, and 5) showed more surface roughness reductions than internal surfaces (Direction 3,4). The summary of the statistical test results for each individual surface are summarized in Table 2. The Ra data from each surface is not consistent with the assumption that both processing time and rotational speed are significant parameters on resultant surface roughness. The authors assumed the reasons of statistical test failure can be attributed a few sources. A limited number of combinations of processing time and rotational speed were conducted. The initial surface roughness of the printed samples (unfinished) varied significantly. The phenomenon was noticed during the experiment while some as-build samples have much lower or higher surface roughness than average.

Table 2. ANOVA significance for Ra values of each surface profile, for both speed and duration and using a significance level of $\alpha=0.05$

Surface (Ra)	RPM Significance ($\alpha=0.05$)	Time Significance ($\alpha=0.05$)
1	Significant	Insignificant
2	Significant	Insignificant
3	Insignificant	Insignificant
4	Significant	Insignificant
5	Insignificant	Insignificant

A categorical regression of all roughness data was then performed, taking into account the measurement location for each sample. The results indicated both surface and measurement location are significant parameters to the resultant surface roughness, at $\alpha=0.05$ significance level. Processes duration (time) was found to not be a significant parameter in this regression test.

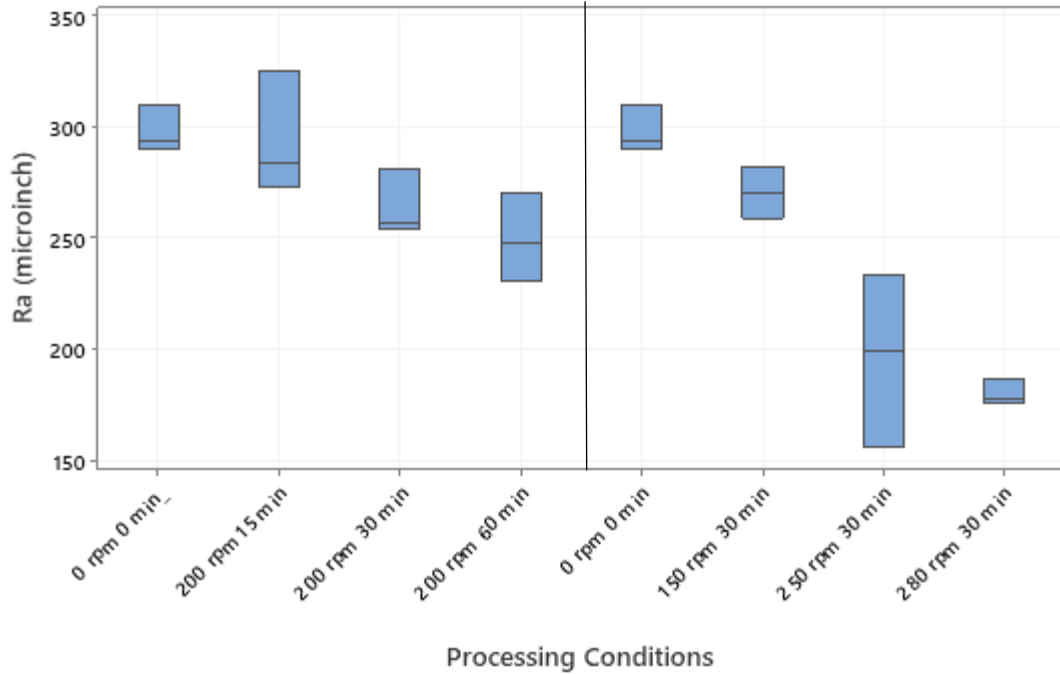


Figure 7. Ra values (μin) for each set of CDF processing conditions for exterior surface parallel to build direction (Direction 1)

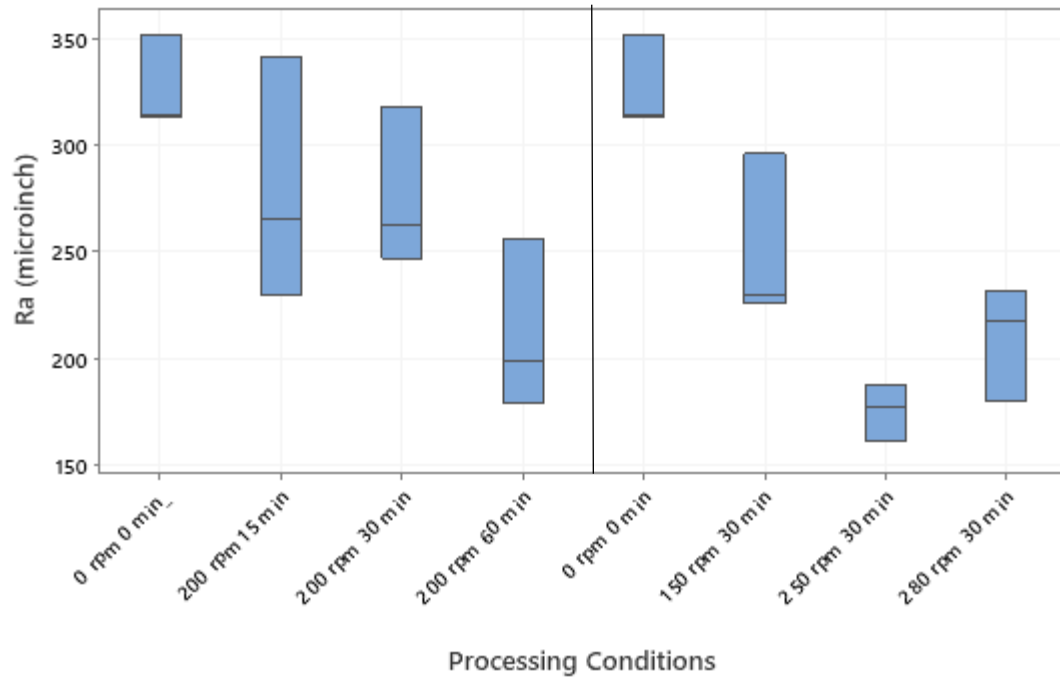


Figure 8. Ra values (μin) for each set of CDF processing conditions for exterior surface perpendicular to build direction (Direction 2)

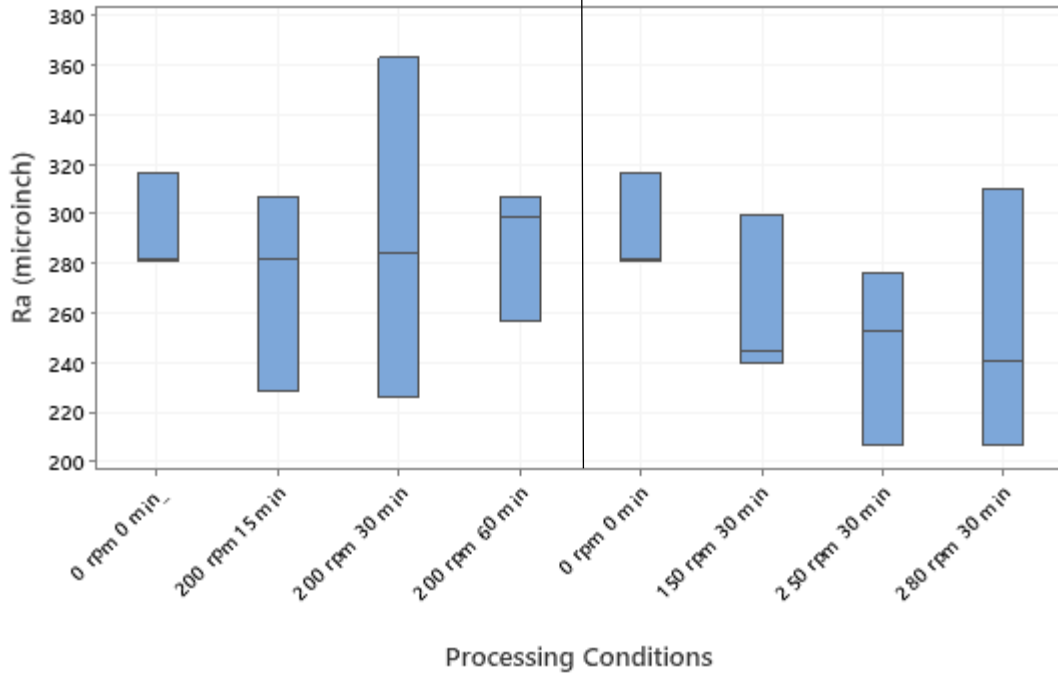


Figure 9. Ra values (μin) for each set of CDF processing conditions for interior tooth surface parallel to build direction (Direction 3)

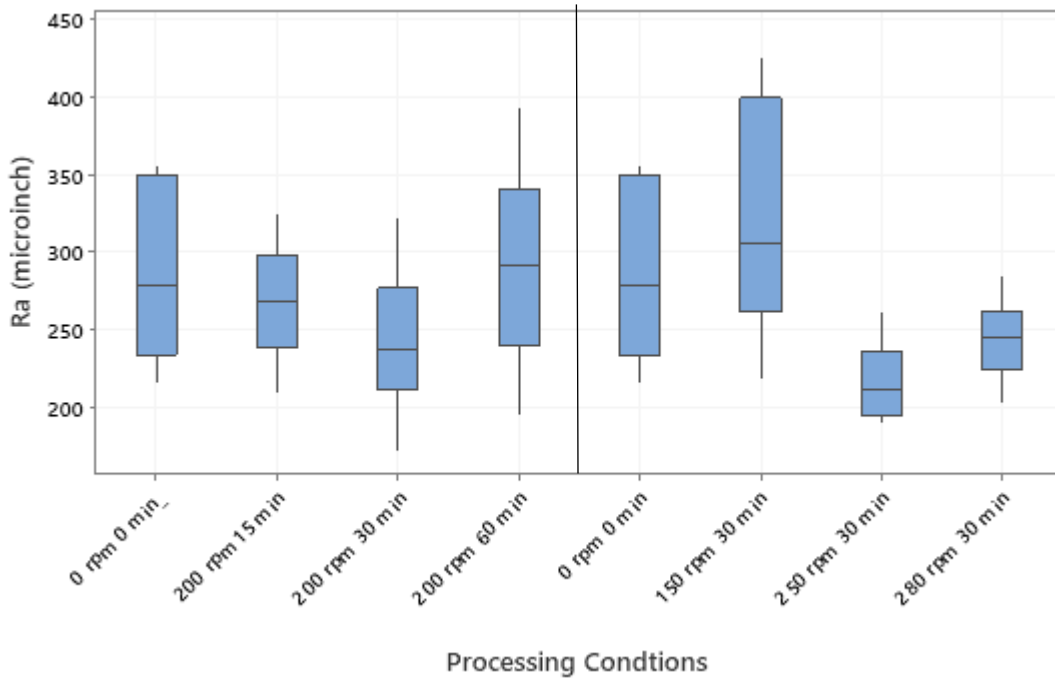


Figure 10. Ra values (μin) for each set of CDF processing conditions for interior tooth surface perpendicular to build direction (Direction 4)

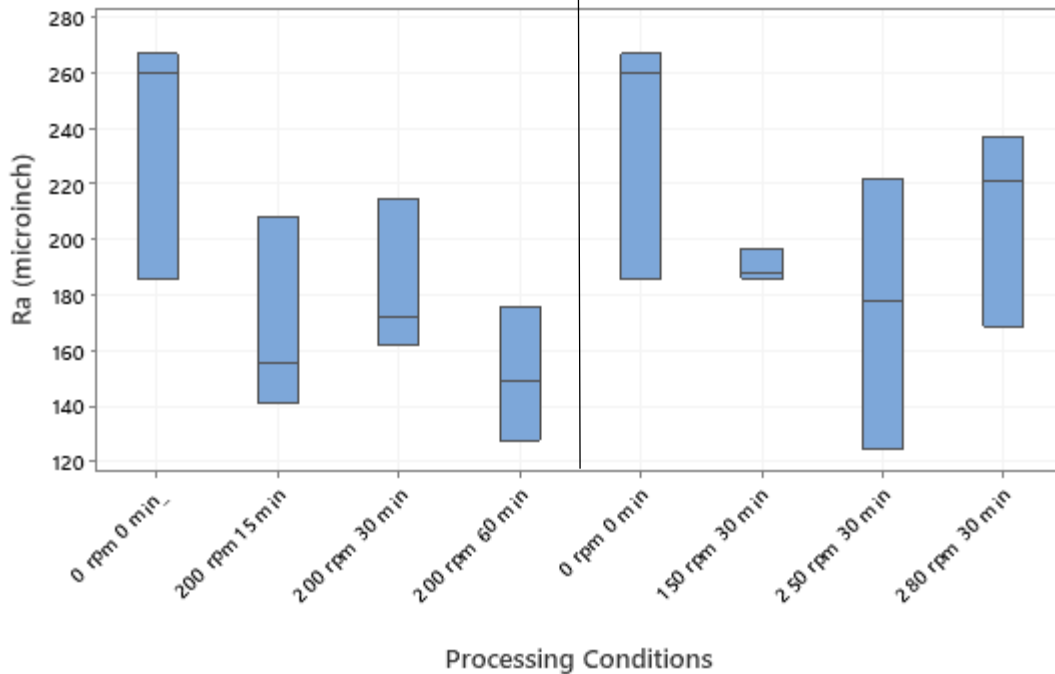


Figure 11. Ra values (μin) for each set of CDF processing conditions for exterior tooth surface parallel to build direction (Direction 5)

Individual Surface Regression Results (Rz)

Similarly, the individual surface roughness data (Rz) collected for each group of test variable combinations can be seen in Figures 12-16. The linear regression results for Profiles 1 and 4 showed that rotational speed (RPM) was a significant parameter but process duration (minutes) was not significant, at $\alpha=0.05$ significance level (Figures A7 and A10). Regression results for Directions 2 and 5 indicated both rotational speed (RPM) and duration (minutes) were significant parameters, at $\alpha=0.05$ significance level (Figures A8 and A11). Neither rotational speed (RPM) nor duration (minutes) was significant at $\alpha=0.05$ significance level for the Direction 3 (Figure A9). The analytical result of Rz is summarized in Table 3. Although not all individual surfaces regression were consistent with the assumption that both speed and time are significant parameter to resultant surface roughness, the boxplot of Rz showed a greater roughness reduction in comparison to the Ra plots. It also demonstrates the assumption that combination of the highest speed and duration resulted in the greatest decreases in surface roughness. Furthermore, the similar categorical regression with Rz indicated profile location, speed, and processing time are all significant parameters at $\alpha=0.05$ significance level (Figure A12). The result proves that aside from speed and processing time, sample measurement location and direction had significant impact on the surface roughness. Additionally, while abrasive medias were able to reduce the external roughness gradually, the media size used in this experiment may have not been suitable for internal features, like surface 3, which showed least reduction and failed to satisfy all statistical tests. However, the Rz boxplot of surface 3 (Figure 14) did show a noticeable reduction in surface roughness in comparison to as-built samples (Samples 19-21).

Table 3. ANOVA significance for Rz values of each surface profile, for both speed and duration and using a significance level of $\alpha=0.05$

Surface (Rz)	RPM Significance ($\alpha=0.05$)	Time Significance ($\alpha=0.05$)
1	Significant	Insignificant
2	Significant	Significant
3	Insignificant	Insignificant
4	Significant	Insignificant
5	Significant	Significant

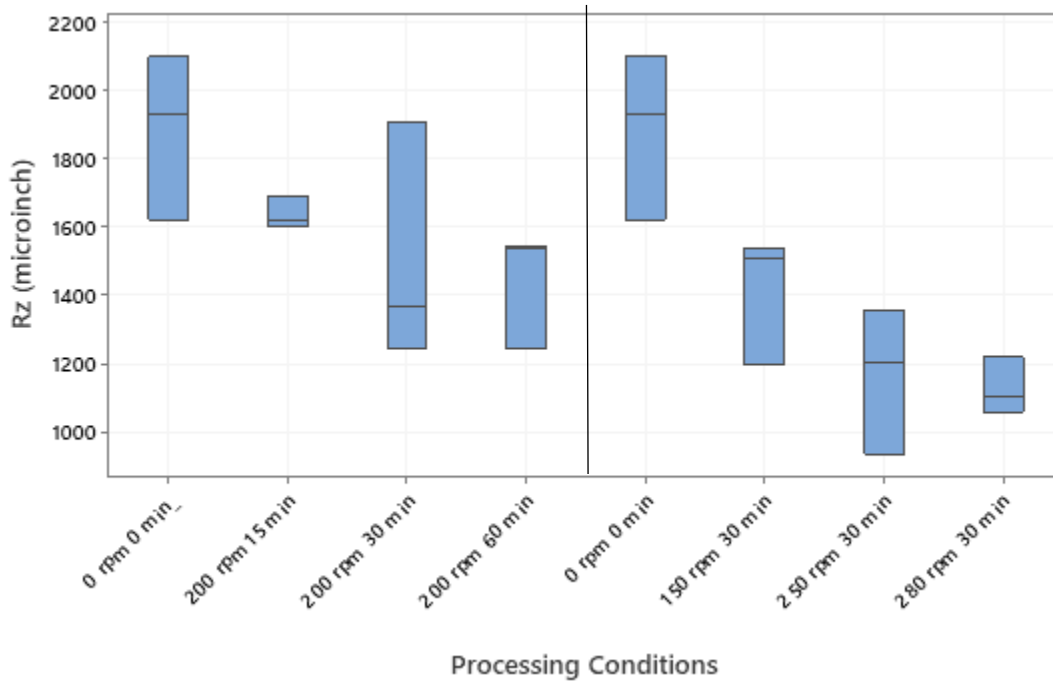


Figure 12. Rz values (μin) for each set of CDF processing conditions for exterior surface parallel to build direction (Direction 1)

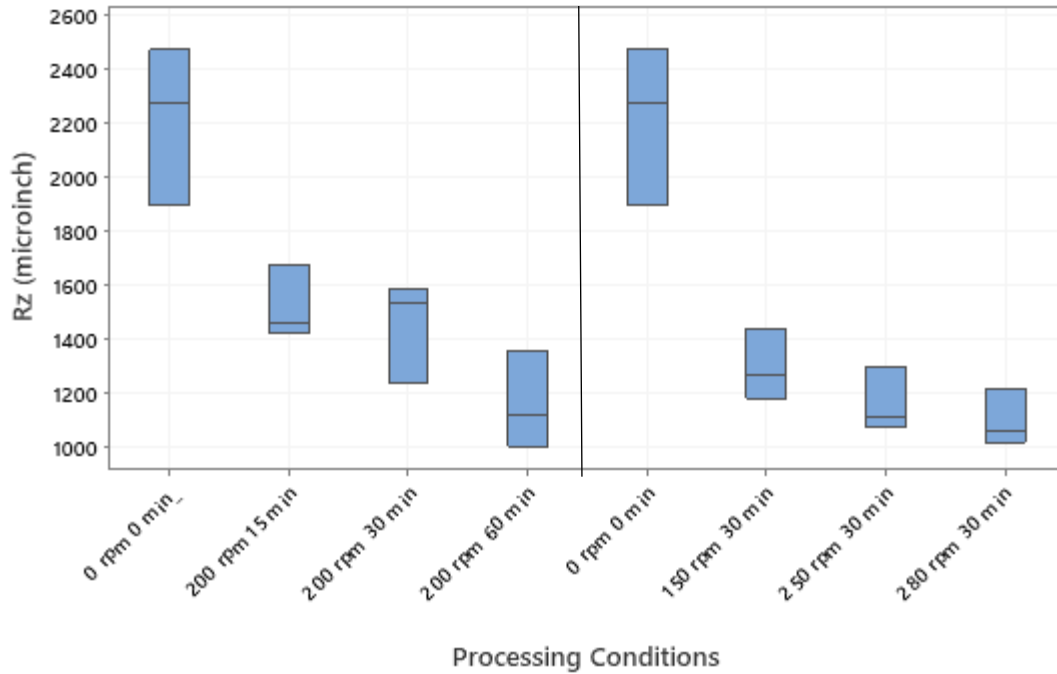


Figure 13. Rz values (μin) for each set of CDF processing conditions for exterior surface perpendicular to build direction (Direction 2)

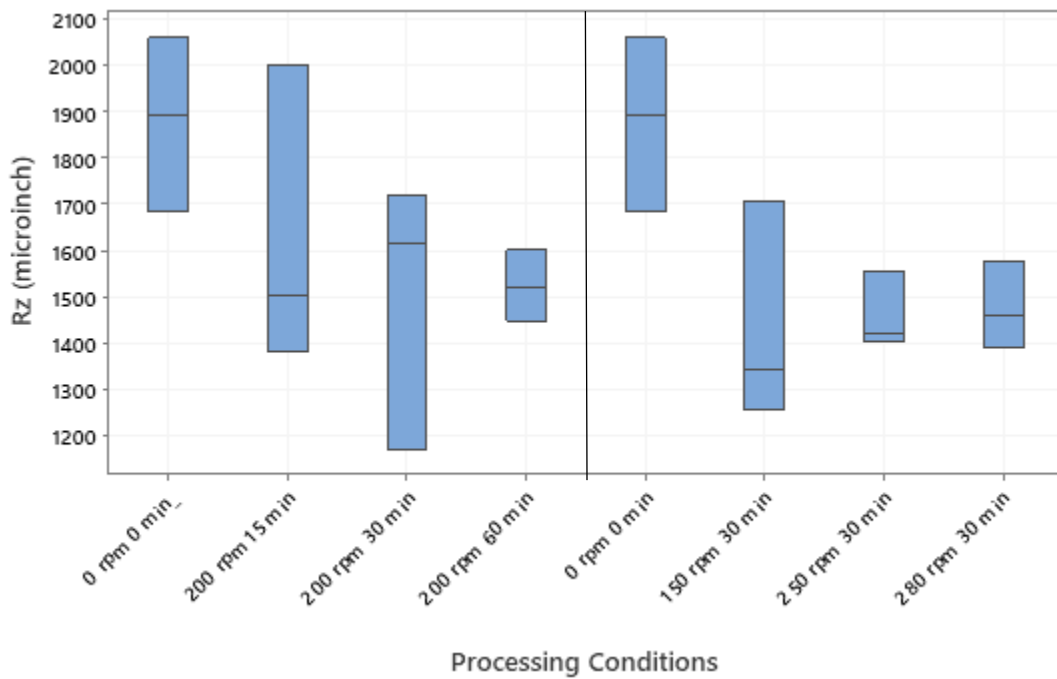


Figure 14. Rz values (μin) for each set of CDF processing conditions for interior tooth surface parallel to build direction (Direction 3)

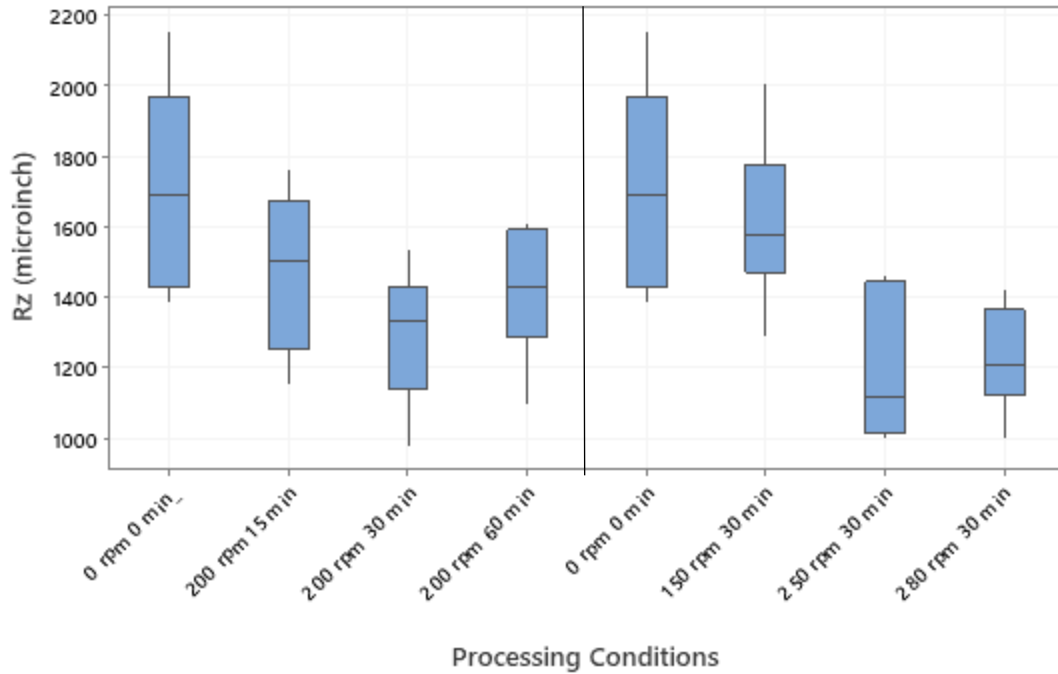


Figure 15. Rz values (μin) for each set of CDF processing conditions for interior tooth surface perpendicular to build direction (Direction 4)

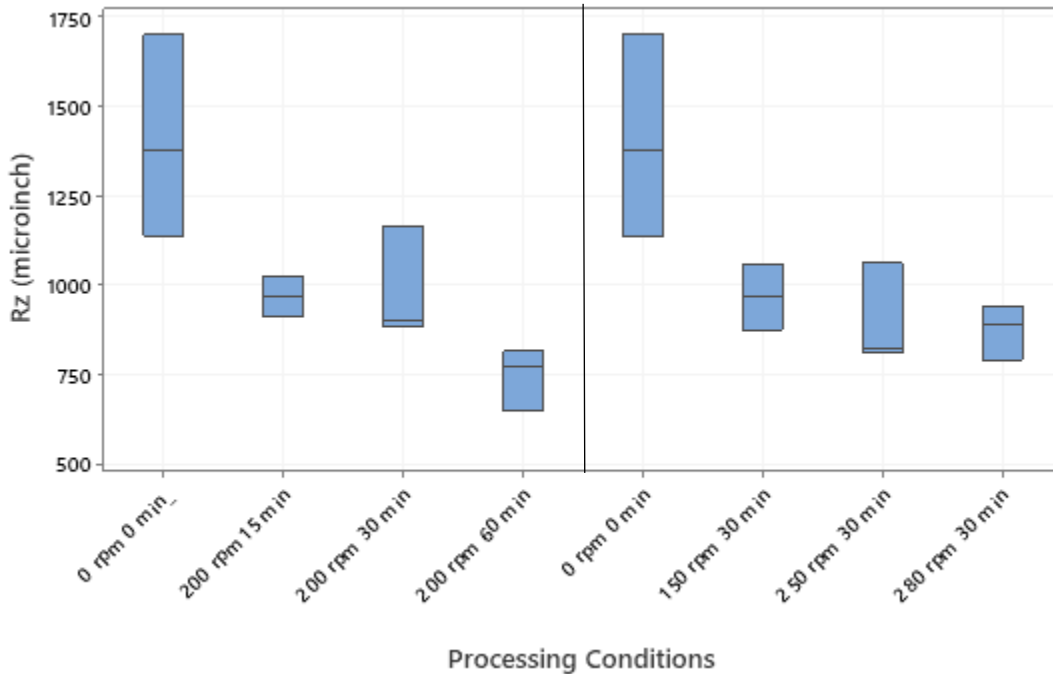


Figure 16. Rz values (μin) for each set of CDF processing conditions for exterior tooth surface parallel to build direction (Direction 5)

The Rz regression analysis demonstrated a significant increase in the R-squared value in comparison to Ra regression result. Furthermore, all predictor parameters were proved significant at 95% confidence level. One cause for the Rz statistical model being better than Ra

model can be attributed to the processes in which CDF smooths the surface by removing “peaks” and leaving “valleys” mostly unaffected. A comparison of the trace profile for Sample 19 (control) and Sample 16 (280 RPM, 30 min) is shown in Figures 17 and 18. It can be seen the profilometer plots that the peaks on Sample 16 are much softer than the sharp ones seen on Sample 19. This same sentiment is corroborated by the CT reconstruction of the same samples in Figure 20. By observing the CT reconstructions, it can be seen that the CDF process dramatically effects the samples’ exterior edges by rounding the sharp corners. Therefore, Rz surface roughness which averages “peak” to “valley” distance on measured surfaces, seems more suitable for comparing this process. The statistical analysis and physical surface profile trace phenomenon demonstrated Rz is a better representation of surface roughness in comparison to Ra.

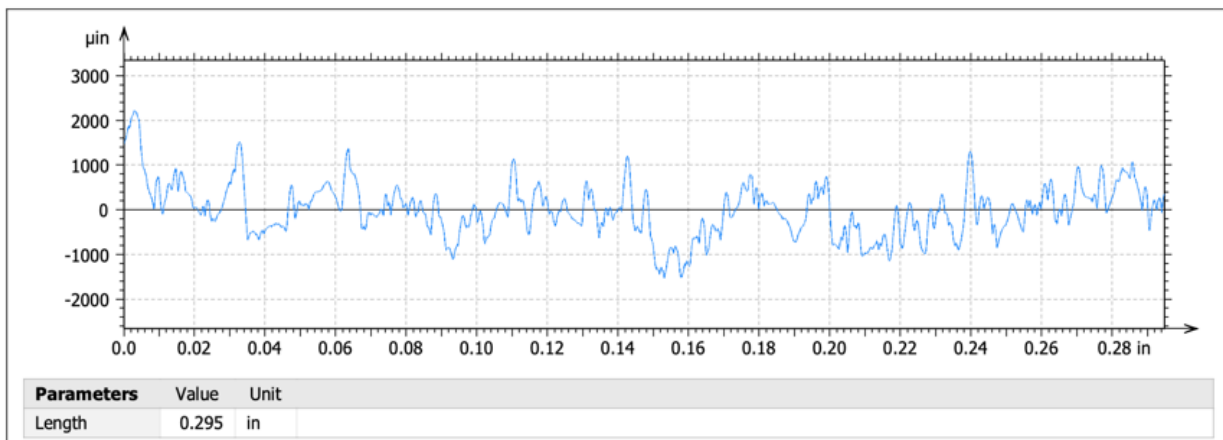


Figure 17. Surface roughness profile for Sample 19 (control) as collected by profilometer

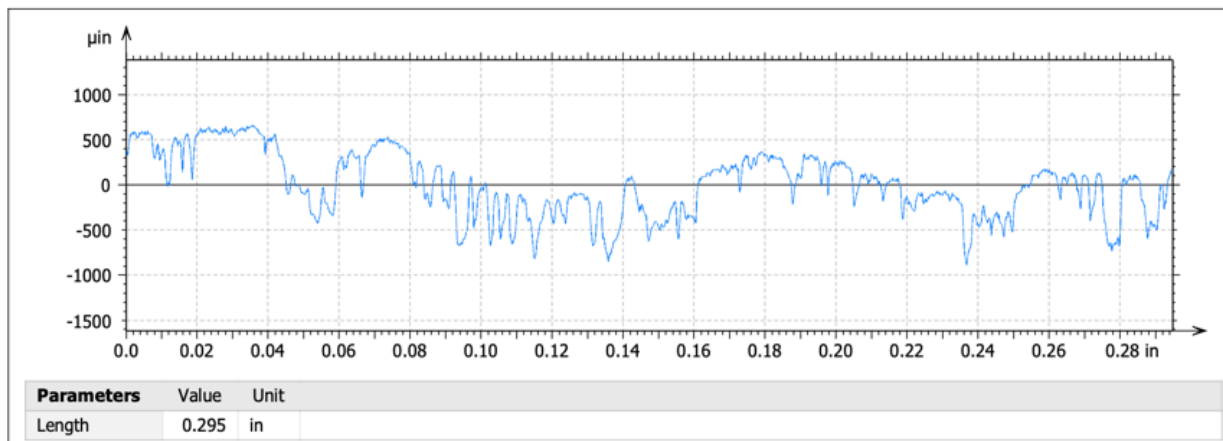


Figure 18. Surface roughness profile for Sample 16 (280 RPM, 30 min) as collected by profilometer

Furthermore, significant lack of fit exists through all statistical analysis, which conclude that linear regression might not be suitable for this study. The CT scanned samples were

reconstructed to visualize surface roughness change under different processing conditions. (Figure 19) The reconstructed images showed much more surface smoothing effect on the edges, while higher speed and longer time processing condition showed more aggressive surface smoothing effect on both surfaces and edges.

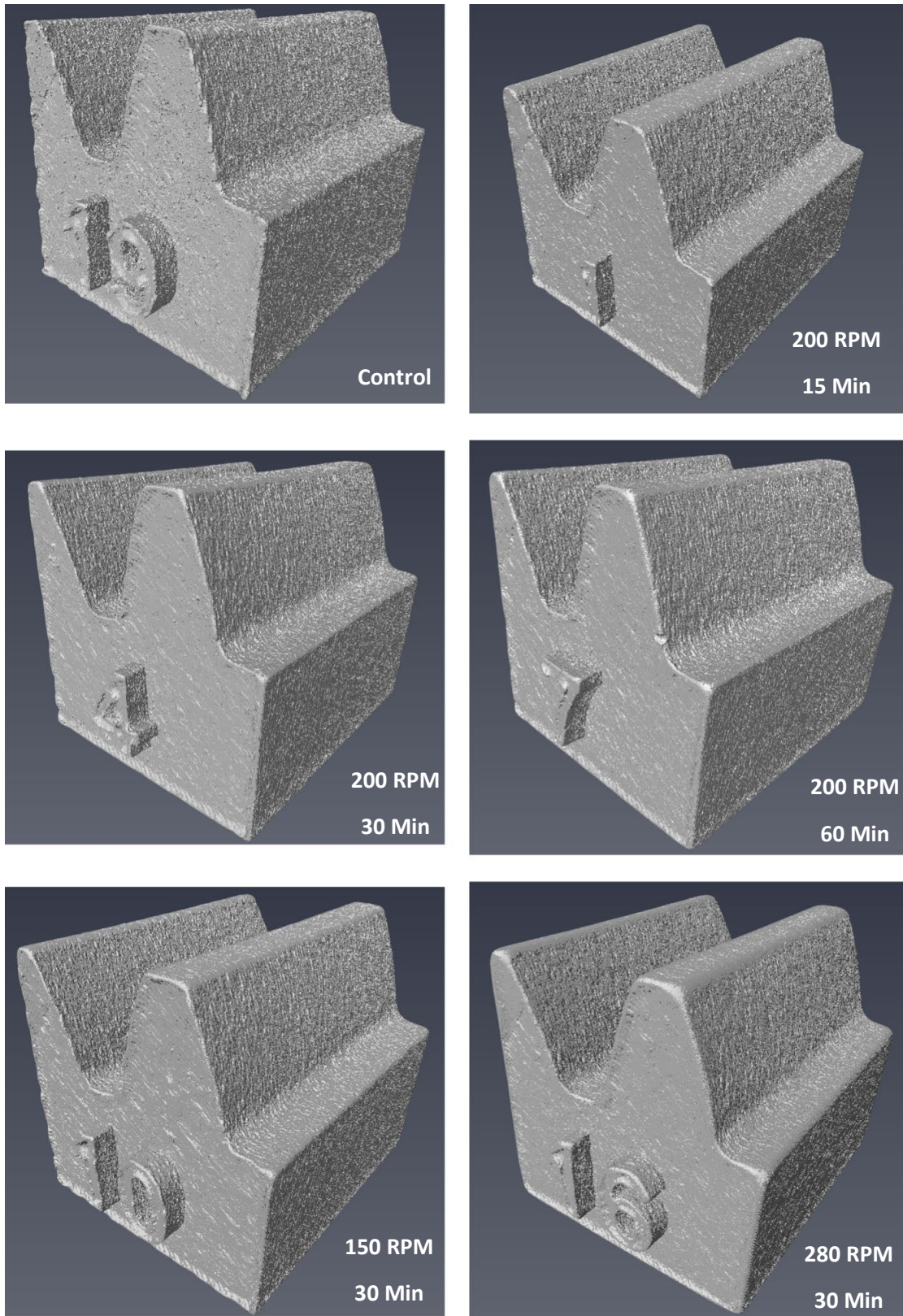


Figure 19. CT reconstructions of select gear teeth samples after CDF processing

Mechanical Test

It is common knowledge in conventional metal manufacturing that fatigue strength can be enhanced by improving surface finish. To understand if the same principle is applicable for Additively Manufactured Ti6Al4V samples, Single Tooth Bending Fatigue (STBF) Gear Test (Modification of SAE J1619) was performed. Gear samples that finished under 200 RPM 15 min condition were Electro Discharge Machined(EDM) into single gear teeth. The testing setup is shown in Figure 20(a)&(b). The bending test machines used was 100 kN Servo-hydraulic Universal Test Machine with 30 Hz test frequency.

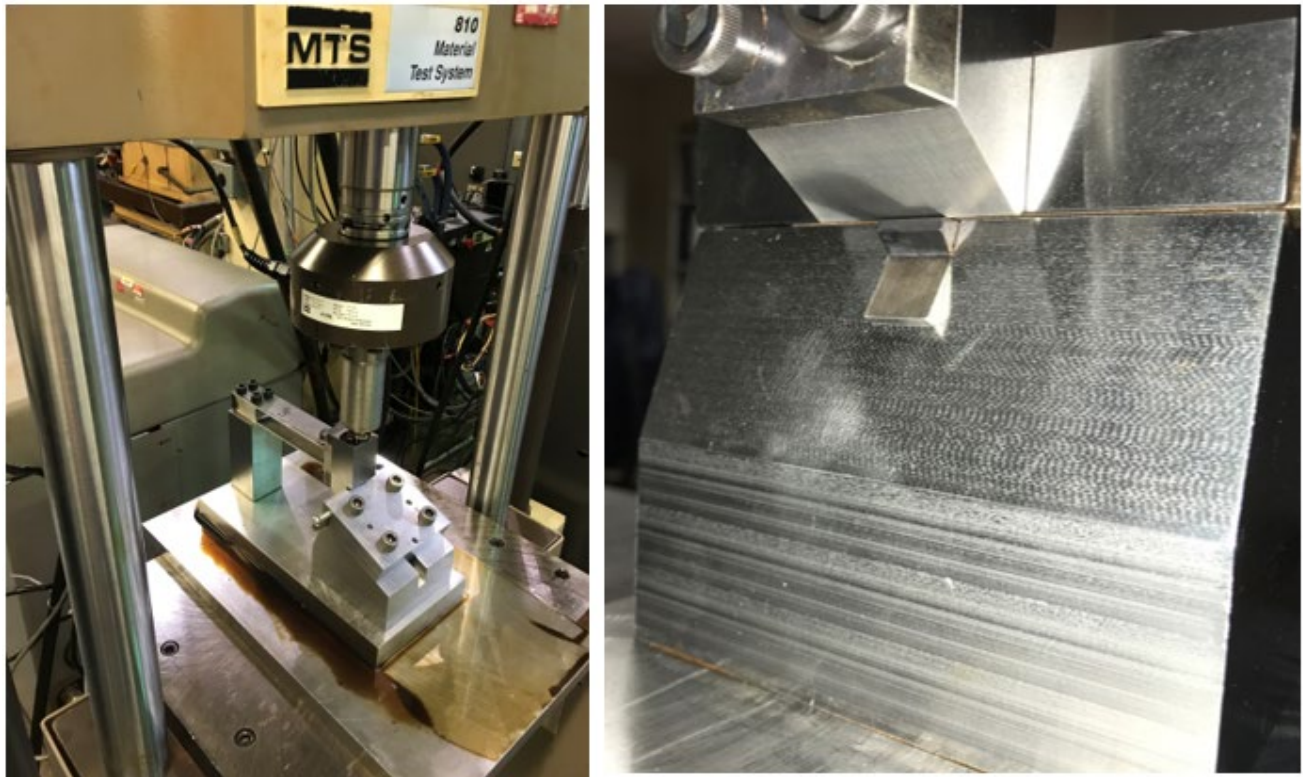


Figure 20. STBF Test Setup: (a) Servo-hydraulic Bending Fatigue Test Machine (b) Gear Tooth in fixture

Three samples were tested. The first sample was tested with a maximum bending stress of 200 MPa and did not fail in 2,000,000 cycles. The second sample was tested under 400 MPa bending stress and a crack was observed at 241,650 cycles on the root fillet on the opposite side of the tooth from the test fillet. This root is loaded in compression., see Figure 21. The same phenomenon occurred in Test 3 with the sample loaded to 500 MPa at approximately 250,000 cycles. In conventionally manufactured gears, the crack should initiate at the tensile side (the same side where load is applied). However, this unexpected behavior of crack initiation on compressive side calls for further metallurgical characterization. It is possible that the AM build contained porosity and/or intermetallic phases that are not typical in conventional gear materials. These defects could be susceptible to failure (crack initiation and growth) under compression that is not typical in wrought materials.

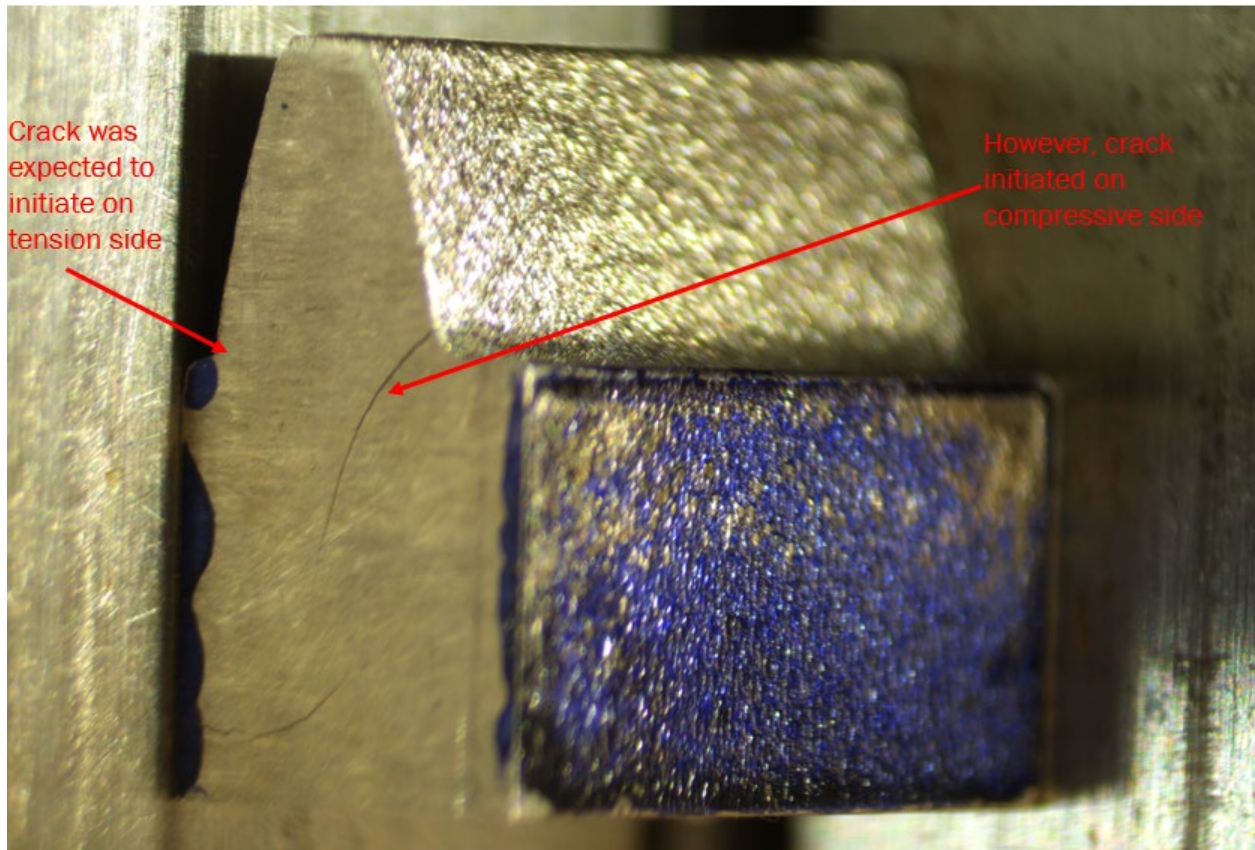


Figure 21. Crack initiated on compressive side unexpectedly under 400 and 500 MPa.

Conclusions & Future Work

The overall regression analysis for Ra values showed the location of measurement and rotational speed were significant parameters, while processing duration was not significant, using a 95% confidence level. However, this can be attributed to limited variable combinations and the range of duration values used not being as wide as the set of rotational speed values. The overall regression for Rz showed that location of measurement, rotational speed, and processing duration were all significant predictors for surface roughness response, for the same confidence level. The profilometer profile trace showed significant reduction and rounding of sharp peaks. CT image reconstruction of the gear samples also showed a noticeable rounding of sharp exterior corners. Although there was no direct relationship observed between the CT and profilometer data, it was determined that higher rotational speed and longer processing time resulted in lower surface roughness for both measurements. In consideration together with the regression result, Rz showed more roughness reduction and better statistical model reliability in comparison to Ra. However, linear regression showed high level of lack of fit in this study.

The result has proved CDF applicability in surface improvement for AM external features. However, further work is needed to better optimization the process. This experiment only considered rotational speed and processing duration as predictors, while literature have shown other parameters such as loading ratio, media geometry/size, workpiece hardness, and lubricant flow rate to be significant in final surface roughness. For future work, further statistical analysis is needed to investigate more predictors and their interaction to determine an optimized material removal rate and surface roughness prediction model. Furthermore, geometric dimensions and tolerances need to be investigated for CDF processed AM parts so that the geometric dimensions and material removal relationship can be interpreted. Further investigation on AM gear material properties is also needed to explain the unexpected fatigue test behavior.

Acknowledgement

The authors acknowledge Penn State Gear Research Institute and Center for Quantitative Imaging for experiment preparation and data collection. The acknowledgement also goes to Ankit Saxena, Nick Carrier, and Phillip King for contribution in experiment.

Appendix

Regression Equation

$$Ra(\mu\text{in}) = 319.7 - 0.390 \text{ Rpm} + 0.067 \text{ Time}(\text{min})$$

Coefficients

Term	Coef	SE Coef	T-Value	P-Value	VIF
Constant	319.7	18.8	16.97	0.000	
Rpm	-0.390	0.113	-3.46	0.003	1.50
Time(min)	0.067	0.561	0.12	0.906	1.50

Model Summary

S	R-sq	R-sq(adj)	R-sq(pred)
35.3345	49.03%	43.37%	33.18%

Analysis of Variance

Source	DF	Adj SS	Adj MS	F-Value	P-Value
Regression	2	21621.2	10810.6	8.66	0.002
Rpm	1	14950.8	14950.8	11.97	0.003
Time(min)	1	17.9	17.9	0.01	0.906
Error	18	22473.5	1248.5		
Lack-of-Fit	4	16233.5	4058.4	9.11	0.001
Pure Error	14	6240.0	445.7		
Total	20	44094.7			

Fits and Diagnostics for Unusual Observations

Obs	Ra (uin)	Fit	Resid	Std Resid
1	325.0	242.8	82.2	2.46 R
14	156.0	224.3	-68.3	-2.02 R

R Large residual

Figure A1. ANOVA table for Ra values (μin) of all samples for exterior surface parallel to build direction (Direction 1)

Regression Equation

$$Ra(\mu\text{in}) = 337.1 - 0.342 \text{ Rpm} - 0.985 \text{ Time}(\text{min})$$

Coefficients

Term	Coef	SE Coef	T-Value	P-Value	VIF
Constant	337.1	22.1	15.22	0.000	
Rpm	-0.342	0.132	-2.59	0.019	1.50
Time(min)	-0.985	0.659	-1.49	0.152	1.50

Model Summary

S	R-sq	R-sq(adj)	R-sq(pred)
41.5221	52.85%	47.61%	38.76%

Analysis of Variance

Source	DF	Adj SS	Adj MS	F-Value	P-Value
Regression	2	34781	17391	10.09	0.001
Rpm	1	11539	11539	6.69	0.019
Time(min)	1	3853	3853	2.23	0.152
Error	18	31034	1724		
Lack-of-Fit	4	12782	3195	2.45	0.095
Pure Error	14	18252	1304		
Total	20	65815			

Fits and Diagnostics for Unusual Observations

Obs	Ra(uin)	Fit	Resid	Std Resid
3	341.0	253.8	87.2	2.22 R

R Large residual

Figure A2. ANOVA table for Ra values (μin) of all samples for exterior surface perpendicular to build direction (Direction 2)

Regression Equation

$$Ra(uin) = 293.7 - 0.186 Rpm + 0.447 \text{ Time(min)}$$

Coefficients

Term	Coef	SE Coef	T-Value	P-Value	VIF
Constant	293.7	21.2	13.86	0.000	
Rpm	-0.186	0.127	-1.47	0.159	1.50
Time(min)	0.447	0.630	0.71	0.487	1.50

Model Summary

S	R-sq	R-sq(adj)	R-sq(pred)
39.7269	10.86%	0.96%	0.00%

Analysis of Variance

Source	DF	Adj SS	Adj MS	F-Value	P-Value
Regression	2	3460.9	1730.5	1.10	0.355
Rpm	1	3412.5	3412.5	2.16	0.159
Time(min)	1	793.0	793.0	0.50	0.487
Error	18	28408.0	1578.2		
Lack-of-Fit	4	3300.0	825.0	0.46	0.764
Pure Error	14	25108.0	1793.4		
Total	20	31869.0			

Fits and Diagnostics for Unusual Observations

Obs	Ra(uin)	Fit	Resid	Std Resid
4	363.0	269.8	93.2	2.41 R

R Large residual

Figure A3. ANOVA table for Ra values (μin) of all samples for intterior tooth profile parallel to build direction (Direction 3)

Regression Equation

$$Ra(uin) = 300.6 - 0.346 Rpm + 1.072 \text{ Time(min)}$$

Coefficients

Term	Coef	SE Coef	T-Value	P-Value	VIF
Constant	300.6	20.7	14.51	0.000	
Rpm	-0.346	0.124	-2.79	0.008	1.50
Time(min)	1.072	0.616	1.74	0.090	1.50

Model Summary

S	R-sq	R-sq(adj)	R-sq(pred)
54.9487	16.69%	12.41%	2.29%

Analysis of Variance

Source	DF	Adj SS	Adj MS	F-Value	P-Value
Regression	2	23584	11792	3.91	0.028
Rpm	1	23515	23515	7.79	0.008
Time(min)	1	9130	9130	3.02	0.090
Error	39	117755	3019		
Lack-of-Fit	4	21678	5420	1.97	0.120
Pure Error	35	96077	2745		
Total	41	141339			

Fits and Diagnostics for Unusual Observations

Obs	Ra(uin)	Fit	Resid	Std Resid
10	426.0	280.9	145.1	2.68 R
31	391.0	280.9	110.1	2.04 R

R Large residual

Figure A4. ANOVA table for Ra values (μin) of all samples for intterior tooth profile perpendicular to build direction (Direction 4)

Regression Equation

$$Ra(\mu\text{in}) = 227.5 - 0.073 \text{ Rpm} - 0.948 \text{ Time}(\text{min})$$

Coefficients

Term	Coef	SE Coef	T-Value	P-Value	VIF
Constant	227.5	18.9	12.04	0.000	
Rpm	-0.073	0.113	-0.65	0.526	1.50
Time(min)	-0.948	0.562	-1.69	0.109	1.50

Analysis of Variance

Source	DF	Adj SS	Adj MS	F-Value	P-Value
Regression	2	8548.0	4274.0	3.40	0.056
Rpm	1	525.1	525.1	0.42	0.526
Time(min)	1	3570.0	3570.0	2.84	0.109
Error	18	22599.8	1255.5		
Lack-of-Fit	4	6039.8	1509.9	1.28	0.326
Pure Error	14	16560.0	1182.9		
Total	20	31147.8			

Model Summary

S	R-sq	R-sq(adj)	R-sq(pred)
35.4336	27.44%	19.38%	0.00%

Figure A5. ANOVA table for Ra values (μin) of all samples of exterior tooth profile parallel to build direction (Direction 5)

Method

Categorical predictor coding (1, 0)

Regression Equation

Surface	Equation
1	$Ra = 298.3 - 0.2805 \text{ Rpm} + 0.121 \text{ Time}$
2	$Ra = 295.0 - 0.2805 \text{ Rpm} + 0.121 \text{ Time}$
3	$Ra = 320.0 - 0.2805 \text{ Rpm} + 0.121 \text{ Time}$
4	$Ra = 315.1 - 0.2805 \text{ Rpm} + 0.121 \text{ Time}$
5	$Ra = 235.7 - 0.2805 \text{ Rpm} + 0.121 \text{ Time}$

Coefficients

Term	Coef	SE Coef	T-Value	P-Value	VIF
Constant	298.3	13.5	22.01	0.000	
Rpm	-0.2805	0.0598	-4.69	0.000	1.50
Time	0.121	0.297	0.41	0.685	1.50
Surface					
2	-3.3	14.2	-0.23	0.817	1.67
3	21.7	14.2	1.53	0.128	1.67
4	16.9	12.3	1.38	0.172	2.00
5	-62.6	14.2	-4.42	0.000	1.67

Model Summary

S	R-sq	R-sq(adj)	R-sq(pred)
45.9141	40.01%	36.99%	33.26%

Analysis of Variance

Source	DF	Adj SS	Adj MS	F-Value	P-Value
Regression	6	167340	27890.0	13.23	0.000
Rpm	1	46445	46445.4	22.03	0.000
Time	1	348	348.0	0.17	0.685
Surface	4	103939	25984.7	12.33	0.000
Error	119	250864	2108.1		
Lack-of-Fit	28	88628	3165.3	1.78	0.022
Pure Error	91	162237	1782.8		
Total	125	418204			

Fits and Diagnostics for Unusual Observations

Obs	Ra	Fit	Resid	Std Resid
24	341.0	240.7	100.3	2.25 R
46	363.0	267.5	95.5	2.13 R
71	393.0	266.3	126.7	2.85 R
73	426.0	276.7	149.3	3.30 R
94	391.0	276.7	114.3	2.52 R
103	216.0	315.1	-99.1	-2.23 R

R Large residual

Figure A6. Categorical regression for Ra values (μin) of all samples of all five directions

Regression Equation

$$Rz (\mu\text{in}) = 1925 - 2.393 \text{ Rpm} - 1.15 \text{ Time}(\text{min})$$

Coefficients

Term	Coef	SE Coef	T-Value	P-Value	VIF
Constant	1925	119	16.14	0.000	
Rpm	-2.393	0.713	-3.36	0.004	1.50
Time(min)	-1.15	3.55	-0.32	0.750	1.50

Model Summary

S	R-sq	R-sq(adj)	R-sq(pred)
223.649	51.36%	45.96%	34.97%

Analysis of Variance

Source	DF	Adj SS	Adj MS	F-Value	P-Value
Regression	2	950705	475353	9.50	0.002
Rpm	1	563572	563572	11.27	0.004
Time(min)	1	5253	5253	0.11	0.750
Error	18	900342	50019		
Lack-of-Fit	4	291162	72791	1.67	0.212
Pure Error	14	609180	43513		
Total	20	1851048			

Fits and Diagnostics for Unusual Observations

Obs	Rz (μin)	Fit	Resid	Std Resid
4	1912.0	1411.7	500.3	2.29 R

R Large residual

Figure A7. ANOVA table for Rz values (μin) of all samples for exterior surface parallel to build direction (Direction 1)

Regression Equation

$$Rz (\mu\text{in}) = 2182.6 - 8.24 \text{ Time}(\text{min}) - 2.937 \text{ Rpm}$$

Coefficients

Term	Coef	SE Coef	T-Value	P-Value	VIF
Constant	2182.6	98.2	22.22	0.000	
Time(min)	-8.24	2.92	-2.82	0.011	1.50
Rpm	-2.937	0.587	-5.00	0.000	1.50

Model Summary

S	R-sq	R-sq(adj)	R-sq(pred)
184.163	80.47%	78.30%	71.01%

Analysis of Variance

Source	DF	Adj SS	Adj MS	F-Value	P-Value
Regression	2	2516102	1258051	37.09	0.000
Time(min)	1	269699	269699	7.95	0.011
Rpm	1	848452	848452	25.02	0.000
Error	18	610488	33916		
Lack-of-Fit	4	175613	43903	1.41	0.280
Pure Error	14	434875	31063		
Total	20	3126590			

Figure A8. ANOVA table for Rz values (μin) of all samples for exterior surface perpendicular to build direction (Direction 2)

Regression Equation

$$Rz(\mu\text{in}) = 1832 - 2.75 \text{ Time}(\text{min}) - 1.086 \text{ Rpm}$$

Coefficients

Term	Coef	SE Coef	T-Value	P-Value	VIF
Constant	1832	106	17.21	0.000	
Time(min)	-2.75	3.17	-0.87	0.396	1.50
Rpm	-1.086	0.637	-1.71	0.105	1.50

Model Summary

S	R-sq	R-sq(adj)	R-sq(pred)
199.654	31.03%	23.37%	11.05%

Analysis of Variance

Source	DF	Adj SS	Adj MS	F-Value	P-Value
Regression	2	322876	161438	4.05	0.035
Time(min)	1	30090	30090	0.75	0.396
Rpm	1	116050	116050	2.91	0.105
Error	18	717507	39862		
Lack-of-Fit	4	106419	26605	0.61	0.663
Pure Error	14	611088	43649		
Total	20	1040384			

Fits and Diagnostics for Unusual Observations

Obs	Rz (uin)	Fit	Resid	Std Resid
2	1999.0	1573.7	425.3	2.25 R

R Large residual

Figure A9. ANOVA table for Rz values (μin) of all samples for interior tooth profile parallel to build direction (Direction 3)

Regression Equation

$$Rz(\mu\text{in}) = 1762.7 - 2.043 \text{ Rpm} + 1.03 \text{ Time}(\text{min})$$

Coefficients

Term	Coef	SE Coef	T-Value	P-Value	VIF
Constant	1762.7	83.4	21.14	0.000	
Rpm	-2.043	0.498	-4.10	0.000	1.50
Time(min)	1.03	2.48	0.41	0.681	1.50

Model Summary

S	R-sq	R-sq(adj)	R-sq(pred)
221.110	36.66%	33.41%	25.69%

Analysis of Variance

Source	DF	Adj SS	Adj MS	F-Value	P-Value
Regression	2	1103559	551779	11.29	0.000
Rpm	1	821236	821236	16.80	0.000
Time(min)	1	8401	8401	0.17	0.681
Error	39	1906699	48890		
Lack-of-Fit	4	273928	68482	1.47	0.233
Pure Error	35	1632771	46651		
Total	41	3010258			

Fits and Diagnostics for Unusual Observations

Obs	Rz (uin)	Fit	Resid	Std Resid
31	2006.0	1487.1	518.9	2.39 R

R Large residual

Figure A10. ANOVA table for Rz values (μin) of all samples for interior tooth profile perpendicular to build direction (Direction 4)

Regression Equation

$$Rz(\mu\text{in}) = 1378.1 - 1.237 \text{ Rpm} - 6.27 \text{ Time}(\text{min})$$

Coefficients

Term	Coef	SE Coef	T-Value	P-Value	VIF
Constant	1378.1	71.9	19.18	0.000	
Rpm	-1.237	0.430	-2.88	0.010	1.50
Time(min)	-6.27	2.14	-2.93	0.009	1.50

Model Summary

S	R-sq	R-sq(adj)	R-sq(pred)
134.755	69.03%	65.59%	50.61%

Analysis of Variance

Source	DF	Adj SS	Adj MS	F-Value	P-Value
Regression	2	728453	364227	20.06	0.000
Rpm	1	150443	150443	8.28	0.010
Time(min)	1	156159	156159	8.60	0.009
Error	18	326859	18159		
Lack-of-Fit	4	29146	7286	0.34	0.845
Pure Error	14	297713	21265		
Total	20	1055313			

Fits and Diagnostics for Unusual Observations

Obs	Rz (uin)	Fit	Resid	Std Resid
19	1137.0	1378.1	-241.1	-2.11 R
20	1700.0	1378.1	321.9	2.82 R

R Large residual

Figure A11. ANOVA table for Rz values (μin) of all samples for exterior tooth profile parallel to build direction (Direction 5)

Method

Categorical predictor coding (1, 0)

Regression Equation

Surface	Regression Equation
1	$Rz(\mu\text{in}) = 1888.9 - 1.956 \text{ Rpm} - 2.73 \text{ Time}(\text{min})$
2	$Rz(\mu\text{in}) = 1849.8 - 1.956 \text{ Rpm} - 2.73 \text{ Time}(\text{min})$
3	$Rz(\mu\text{in}) = 1990.6 - 1.956 \text{ Rpm} - 2.73 \text{ Time}(\text{min})$
4	$Rz(\mu\text{in}) = 1851.4 - 1.956 \text{ Rpm} - 2.73 \text{ Time}(\text{min})$
5	$Rz(\mu\text{in}) = 1411.0 - 1.956 \text{ Rpm} - 2.73 \text{ Time}(\text{min})$

Coefficients

Term	Coef	SE Coef	T-Value	P-Value	VIF
Constant	1888.9	62.4	30.29	0.000	
Rpm	-1.956	0.275	-7.11	0.000	1.50
Time(min)	-2.73	1.37	-1.99	0.049	1.50
Surface					
2	-39.1	65.2	-0.60	0.550	1.67
3	101.7	65.2	1.56	0.122	1.67
4	-37.5	56.5	-0.66	0.508	2.00
5	-477.9	65.2	-7.33	0.000	1.67

Model Summary

S	R-sq	R-sq(adj)	R-sq(pred)
211.338	62.95%	61.08%	58.29%

Analysis of Variance

Source	DF	Adj SS	Adj MS	F-Value	P-Value
Regression	6	9031578	1505263	33.70	0.000
Rpm	1	2259458	2259458	50.59	0.000
Time(min)	1	177097	177097	3.97	0.049
Surface	4	4262980	1065745	23.86	0.000
Error	119	5314994	44664		
Lack-of-Fit	28	1729366	61763	1.57	0.058
Pure Error	91	3585628	39403		
Total	125	14346571			

Fits and Diagnostics for Unusual Observations

Obs	Rz (uin)	Fit	Resid	Std Resid
4	1912.0	1415.9	496.1	2.41 R
40	2476.0	1849.8	626.2	3.10 R
41	2278.0	1849.8	428.2	2.12 R
44	1999.0	1558.4	440.6	2.15 R
94	2006.0	1476.2	529.8	2.54 R
103	1386.0	1851.4	-465.4	-2.28 R

R Large residual

Figure A12. Categorical regression for Rz values (μin) of all samples of all five directions

References

1. Thomas DS, Gilbert SW (2015) Costs and cost effectiveness of additive manufacturing: A literature review and discussion. Nova Science Publishers, Inc., Gaithersburg, MD
2. (2019) Wohlers Report 2019. Fort Collins, Colorado
3. Tulinski EH (1994) Mass finishing. *ASM Handb* 5:118–125
4. Kitajima K, Yamamoto A, Takahashi S, Watanabe M (2009) Finishing characteristics in barrel finishing of centrifugal disc type on flow-through system. *Adv Mater Res* 76–78:300–305. <https://doi.org/10.4028/www.scientific.net/AMR.76-78.300>
5. Matsumoto Y, Yamaguchi T, Kitajima K, et al (2014) Study on the flow pressure of mass in centrifugal disc finishing. *Adv Mater Res* 1017:559–564. <https://doi.org/10.4028/www.scientific.net/AMR.1017.559>
6. Sutowski P, Plichta J, Kałduński P (2019) Determining kinetic energy distribution of the working medium in a centrifugal disc finishing process—part 1: theoretical and numerical analysis with DEM method. *Int J Adv Manuf Technol* 104:1345–1355. <https://doi.org/10.1007/s00170-019-03872-2>
7. Sutowski P, Plichta J, Kałduński P (2019) Determining kinetic energy distribution of the working medium in a centrifugal disc finishing process—part 2: experimental analysis with the use of acoustic emission signal. *Int J Adv Manuf Technol* 104:687–704. <https://doi.org/10.1007/s00170-019-03937-2>
8. Cariapa V, Park H, Kim J, et al (2008) Development of a metal removal model using spherical ceramic media in a centrifugal disk mass finishing machine. *Int J Adv Manuf Technol* 39:92–106. <https://doi.org/10.1007/s00170-007-1195-5>
9. Domblesky J, Evans R, Cariapa V (2004) Material removal model for vibratory finishing. *Int J Prod Res* 42:1029–1041. <https://doi.org/10.1080/00207540310001619641>
10. Uhlmann E, Dethlefs A, Eulitz A (2014) Investigation into a geometry-based model for surface roughness prediction in vibratory finishing processes. *Int J Adv Manuf Technol* 75:815–823. <https://doi.org/10.1007/s00170-014-6194-8>
11. Mullany B, Shahinian H, Navare J, et al (2017) The application of computational fluid dynamics to vibratory finishing processes. *CIRP Ann - Manuf Technol* 66:309–312. <https://doi.org/10.1016/j.cirp.2017.04.087>
12. Makiuchi Y, Hashimoto F, Beaucamp A (2019) Model of material removal in vibratory finishing, based on Preston's law and discrete element method. *CIRP Ann* 68:365–368. <https://doi.org/10.1016/j.cirp.2019.04.082>
13. Vijayaraghavan V, Castagne S, Srivastava S, Qin CZ (2017) State-of-the-art in experimental and numerical modeling of surface characterization of components in mass finishing process. *Int J Adv Manuf Technol* 90:2885–2899. <https://doi.org/10.1007/s00170-016-9595-z>
14. Jamal M, Morgan MN (2017) Design process control for improved surface finish of metal additive manufactured parts of complex build geometry. *Inventions* 2:. <https://doi.org/10.3390/inventions2040036>
15. Boschetto A, Bottini L, Veniali F (2018) Surface roughness and radiusing of Ti6Al4V selective laser melting-manufactured parts conditioned by barrel finishing. *Int J Adv Manuf Technol* 94:2773–2790. <https://doi.org/10.1007/s00170-017-1059-6>
16. Townsend A, Senin N, Blunt L, et al (2016) Surface texture metrology for metal additive manufacturing: a review. *Precis Eng* 46:34–47. <https://doi.org/10.1016/j.precisioneng.2016.06.001>